Journal of Power Sources 268 (2014) 517–521

Contents lists available at ScienceDirect

Journal of Power Sources

journal homepage: www.elsevier.com/locate/jpowsour

Short communication

Temperature dependence of the initial coulombic efficiency in Li-rich layered $Li[Li_{0.144}Ni_{0.136}Co_{0.136}Mn_{0.544}]O_2$ oxide for lithium-ions batteries

Bao Qiu [a], Jun Wang [b], Yonggao Xia [a, *], Zhen Wei [a], Shaojie Han [a], Zhaoping Liu [a, *]

[a] Ningbo Institute of Materials Technology & Engineering (NIMTE), Chinese Academy of Sciences, Ningbo, Zhejiang 315201, PR China
[b] MEET Battery Research Center/Institute of Physical Chemistry, University of Muenster, Corrensstrasse 46, 48149 Muenster, Germany

HIGHLIGHTS

- The ICE for Li-rich layered oxides is significantly dependent on the testing temperature.
- The lithium intercalation into MnO_2-like component greatly dominates the ICE.
- The ICE reproducibly approaches 92% when discharged at 50 °C regardless of charging temperature.

ARTICLE INFO

Article history:
Received 7 January 2014
Received in revised form
30 May 2014
Accepted 5 June 2014
Available online 25 June 2014

Keywords:
Lithium-rich oxide
Temperature
Initial coulombic efficiency
Manganese dioxide-like component

ABSTRACT

In this study we report on the temperature dependence of the initial coulombic efficiency (ICE) in Li-rich layered $Li[Li_{0.144}Ni_{0.136}Co_{0.136}Mn_{0.544}]O_2$ oxide, consisting of rhombohedral $LiNi_{1/3}Co_{1/3}Mn_{1/3}O_2$ and monoclinic Li_2MnO_3 component confirmed by SXRD and SAED. The electrochemical result shows that the ICE increases from 74.6 to 91.5% with the applied charging/discharging temperature from 0 to 50 °C, and it reproducibly approaches 92% when discharged at 50 °C, regardless of the applied charging temperature. From the d*Q*/d*V* plots, it is observed that the discharging temperature significantly influences the lithium intercalation into the MnO_2-like component derived from Li_2MnO_3 component, *i.e.* the discharge process determines the ICE. This phenomenon indicates that the lithium re-intercalation into the MnO_2-like component appears to be the most important factor.

1. Introduction

At present, electrode materials for rechargeable lithium-ion batteries with high energy density to be used in mobile electronics and electric vehicles are under development worldwide [1]. For this purpose, high energy density is readily available using layered Li-rich oxide (xLi_2MnO_3–$(1-x)LiMO_2$, M = Ni, Co, Mn [2,3]) as cathode material, exhibiting high specific capacities of more than 250 mAh g^{-1} when cycled above 4.6 V. However, this kind of material suffers from a large initial irreversible capacity loss, *i.e.* a low initial coulombic efficiency (ICE) [2–4]. It is more likely that this kind of material can be considered as two components of Li_2MnO_3 (*C2/m*) and $LiMO_2$ (*R-3m*) than as a homogeneous solid solution [5]. Moreover, the ICE value of the layered Li-rich oxide is closely related to the activation of the Li_2MnO_3 component in the initial charge process, which is largely dependent on the composition [4], charge cut-off voltage [6], current density [7], and so on [8,9].

The reason for the low ICE of the layered Li-rich oxide is still under debate. In general, the main reason for the low ICE is caused by the oxygen loss during the initial charging process when the cut-off voltage is above 4.5 V, which leads to oxygen vacancies forming in the lattice [10]. During the discharge process, only a part of the extracted lithium can reintercalate into the MnO_2-like component [4]. This mechanism could well explain the charge plateau at about 4.5 V and the low ICE [2], but be unable to explain the obtained high capacity [11]. Recently, Ohzuku et al. found a significant increase in the ICE, when the cell was cycled at elevated temperature [11]. Furthermore, calculated by energy activation equation, it was shown that the lithium intercalation process into MnO_2-like component is more sensitive to temperature [12]. This indicates that the reintercalation process into the MnO_2-like component might thermodynamically affect the ICE of the Li-rich layered

* Corresponding authors. Tel./fax: +86 574 8668 5096.
E-mail addresses: xiayg@nimte.ac.cn (Y. Xia), liuzp@nimte.ac.cn (Z. Liu).

http://dx.doi.org/10.1016/j.jpowsour.2014.06.031
0378-7753/

oxides. In this communication, we focus on investigating the role of temperature on influencing the response of the lithium re-intercalation into the MnO_2-like component to the ICE of Li-rich layered $Li[Li_{0.144}Ni_{0.136}Co_{0.136}Mn_{0.544}]O_2$ oxides.

2. Experimental

Li-rich layered oxide with a nominal formula $Li[Li_{0.144}Ni_{0.136}Co_{0.136}Mn_{0.544}]O_2$ was synthesized through solid-state reaction between Li_2CO_3 and $(Ni_{1/6}Co_{1/6}Mn_{4/6})CO_3$ powders. The molar ratio between them was set to 0.7. The mixed precursor was firstly pre-treated at 500 °C for 5 h and then calcined at 850 °C for 15 h. The detailed synthesis process of the $(Ni_{1/4}Co_{1/4}Mn_{4/6})CO_3$ precursor using co-precipitation method was described in our previous work [13]. For the investigation of the electrochemical properties of the layered Li-rich oxide coin cells (type CR2032) were fabricated. The cathode was prepared by casting a slurry of the active material (80 *wt.* %), conductive graphite (Super P, 10 *wt.* %), and binder (polyvinylidene fluoride, 10 *wt.* %) in N-methyl-2-pyrrolidone (NMP) on aluminum foil. Celgard 2502 was utilized as separator. A mixture of ethylene and dimethyl carbonate (3:7 *vol.* ratio) with $LiPF_6$ (1 M) was used as electrolyte. Lithium metal was employed as counter electrode. The loading density of the active material on the electrode was around 6.0 mg cm^{-2}. Unless otherwise specified, the cells were cycled between 2.0 and 4.6 V *versus* Li^+/Li^0 with the current density of 25 mA g^{-1} at various operating temperatures. The temperature stability for the tests was controlled within 0.5 °C. The active material powder was characterized using synchrotron X-ray diffraction (SXRD, Beamline BL14B1 of Shanghai Synchrotron Radiation Facility, with a wavelength of 1.2398 Å) and field emission scanning electron microscopy (FESEM, Hitachi S-4800) and selected area electron diffraction (SAED, FEI Tecnai G2 F20). SXRD data were recorded in the 2θ range between 10° and 85°.

3. Results and discussion

Fig. 1(a) shows SXRD pattern of the obtained layered $Li[Li_{0.144}Ni_{0.136}Co_{0.136}Mn_{0.544}]O_2$. It is obvious that all peaks can be well indexed on the basis of $LiCoO_2$ (space group: *R-3m*) structure except for several weak peaks at around 16°–18°. These peaks originate from the superlattice ordering of Li and Mn in the transition metal layers for the Li-rich layered oxides, which proves the existence of Li_2MnO_3 (*C2/m*) component [7]. The structural composite study of this Li-rich layered oxide material was carried out by Rietveld refinement analysis using GSAS program [14]. The calculated XRD pattern, on the basis of the two-phase model consisting of rhombohedral $LiNi_{1/3}Co_{1/3}Mn_{1/3}O_2$ and monoclinic Li_2MnO_3, was found in good agreement with experimental data (R_{wp} = 6.26%, R_p = 4.89% and χ^2 = 2.217). And the lattice parameters a, c are 2.854 and 14.263 Å with only 3.5% Li/Ni mixing, respectively. Particle size as determined by FESEM (Fig. 1(b)) is between 100 and 200 nm. Additionally, SAED image (Fig. 1(c)) illustrates clear evidence of the coexistence of $LiMO_2$ and Li_2MnO_3 domains and the pattern can be typically regarded as the superposition of a rhombohedral $LiCoO_2$ pattern and three monoclinic Li_2MnO_3 patterns rotated 120° along the [001] axis [5]. These results suggest that this Li-rich layered material can be considered to be a mixture of rhombohedral $LiNi_{1/3}Co_{1/3}Mn_{1/3}O_2$ and monoclinic Li_2MnO_3 component.

Fig. 2(a) shows the initial charge–discharge curves of the cathode material at various operating temperatures. As expected, a long plateau in the charge curve above 4.4 V is observed at all testing temperatures. This is attributed to the electrochemical activation of Li_2MnO_3 component to generate MnO_2-like component [10]. It is noted that the charge capacity of the plateau region remarkably drops with lowering the charging temperature. This

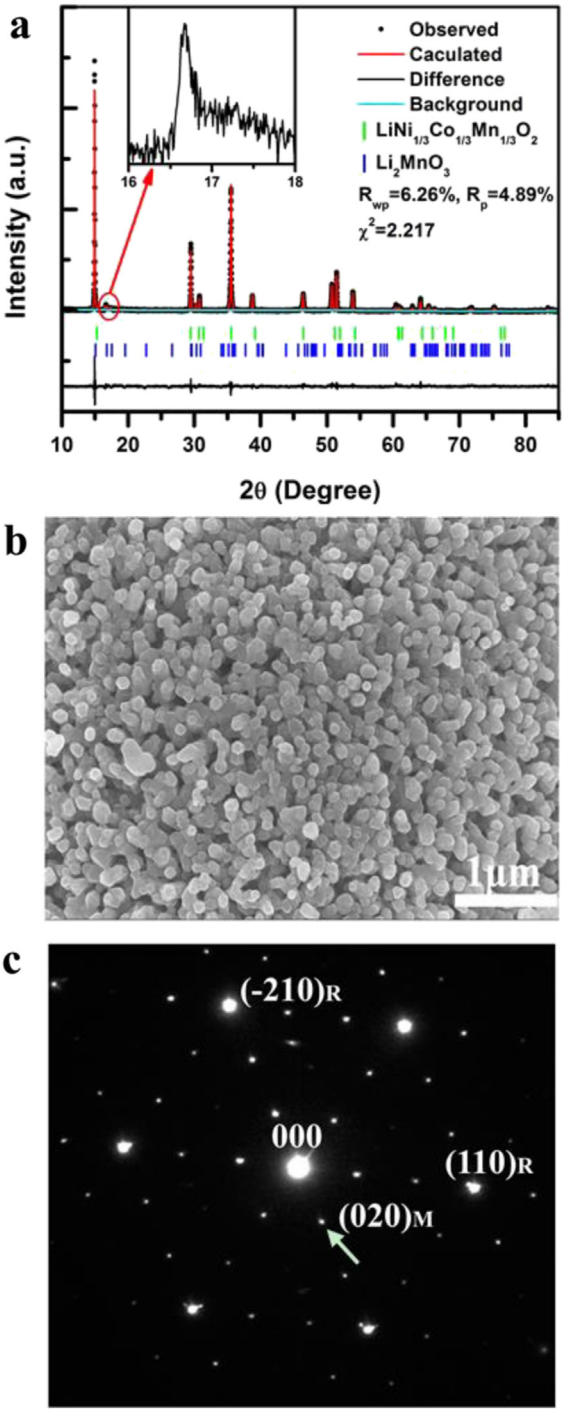

Fig. 1. (a) Synchrotron XRD pattern and Rietveld refinement profile of the Li $[Li_{0.144}Ni_{0.136}Co_{0.136}Mn_{0.544}]O_2$ oxide; (b) FESEM image and (c) SAED image of the Li $[Li_{0.144}Ni_{0.136}Co_{0.136}Mn_{0.544}]O_2$ oxide.

temperature-related trend is most likely associated with the interface reaction impedance increasing [15]. It is known that the less the Li_2MnO_3-like component is initially activated, the lower the initial discharge capacity is acquired, but the higher the ICE is achieved in the material [6,15]. It can be seen from Table 1 that the charge capacity increases from 168.6 to 319.5 mAh g^{-1} with the charging temperature from 0 to 50 °C. Similar trend can be found for the discharge capacity, *i.e.* it increases from 125.2 to 292.1 mAh g^{-1}. Consequently, the ICE increases up to 91.5% at 50 °C,

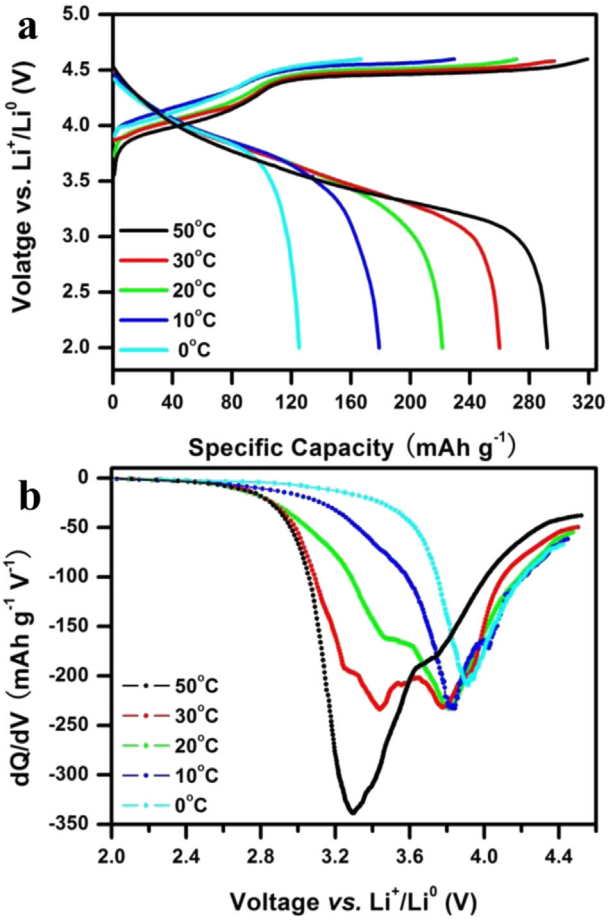

Fig. 2. (a) Initial charge–discharge curves and (b) differential discharge capacity (d*Q*/d*V*) plots of Li-rich layered $Li[Li_{0.144}Ni_{0.136}Co_{0.136}Mn_{0.544}]O_2$ oxide cells under various temperatures. The same testing temperature during the charge and discharge process was carried out.

compared to that of 74.2% at 0 °C. Apparently there is a strong dependence of the ICE on the charging/discharging temperature.

To clearly interpret this contradiction, the discharge differential capacity (d*Q*/d*V*) plots are illustrated in Fig. 2(b). It is clearly observed that the reduction peak at about 3.8 V, which is generally considered as the reduction of Ni^{4+} or Co^{4+} ions in the rhombohedral phase [4], is hardly affected by the testing temperature. In contrast, the other peak at around 3.3 V is significantly dependent on cycling temperature. This peak is assigned to Li^+ intercalation into the layered MnO_2-like component derived from Li_2MnO_3 component [16]. This means that the process about lithium re-intercalation into MnO_2-like component is more sensitive to temperature. In this regard, a part of lithium ions cannot re-intercalate into MnO_2-like component. And this process leads to lower ICE, even though a part of Li_2MnO_3 component has been activated. To illustrate the influence of temperature on this behavior, we further choose two appropriate operating conditions: charging at various temperatures and discharging at 50 °C, charging at 50 °C and discharging at various temperatures. The initial discharge curves and corresponding d*Q*/d*V* plots are presented in Figs. 3 and 4, respectively. In addition, Table 1 illustrates the electrochemical data of Li-rich layered oxide electrode material at various operating temperatures. It is evident that the initial discharge capacity, initial irreversible capacity loss and ICE of this 'composite' layered material are really controlled by operating temperature during the first discharge process. For instance, the discharge capacity value for discharging at 50 °C could reach 250.8 mAh g^{-1} compared to that of 221.4 mAh g^{-1} at 20 °C, even though both were charged at 20 °C. By comparing with two d*Q*/d*V* plots (shown in Figs. 2b and 3b), it is clearly observed that the intensity of the peak at around 3.3 V for the former is larger than that

Table 1
Electrochemical data of Li-rich layered $Li[Li_{0.144}Ni_{0.136}Co_{0.136}Mn_{0.544}]O_2$ oxides at various testing temperatures.

Charge	Discharge	Initial charge capacity (mAh g^{-1})	Initial discharge capacity (mAh g^{-1})	Initial irreversible capacity (mAh g^{-1})	Initial coulombic efficiency (%)
0 °C	0 °C	167.8	125.2	42.5	74.6
	50 °C		156.9	10.9	93.5
10 °C	10 °C	229.5	179.0	50.5	78.0
	50 °C		210.5	19.0	91.7
20 °C	20 °C	271.6	221.4	50.2	81.5
	50 °C		250.8	20.8	91.7
30 °C	30 °C	296.8	259.9	36.9	87.6
	50 °C		271.9	24.9	91.6
50 °C	0 °C	319.1	206.1	103.0	64.6
	10 °C		227.3	91.8	71.2
	20 °C		247.8	71.3	77.6
	30 °C		265.2	53.9	83.1
	50 °C		292.1	27.0	91.5

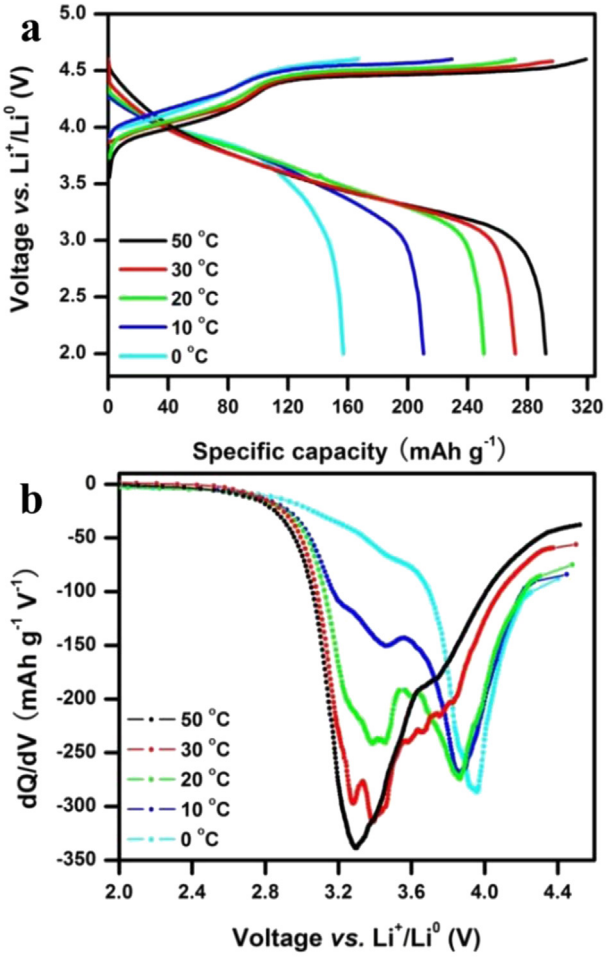

Fig. 3. (a) Initial discharge curves and (b) d*Q*/d*V* plots of Li-rich layered Li $[Li_{0.144}Ni_{0.136}Co_{0.136}Mn_{0.544}]O_2$ oxide cells with different charging temperature and all the discharge process were performed at 50 °C.

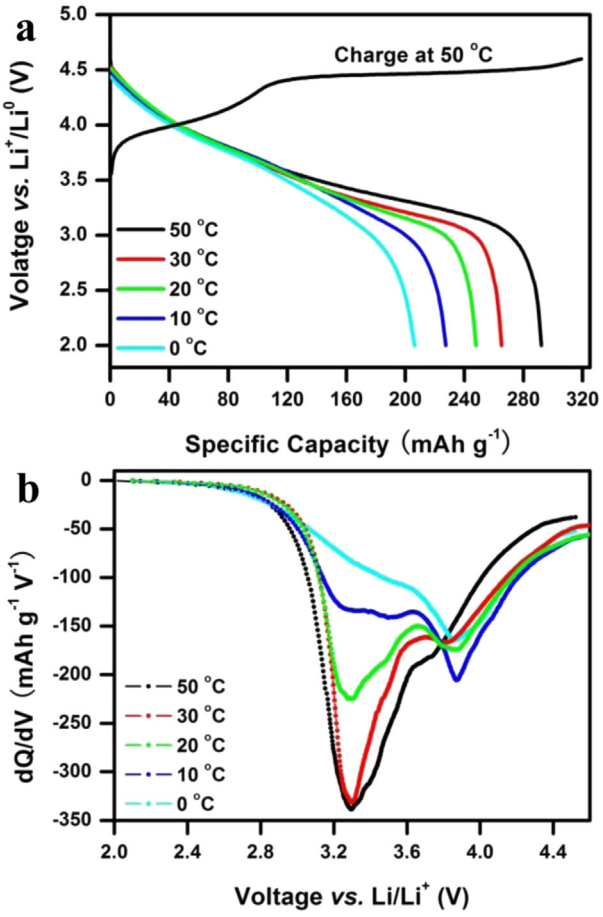

Fig. 4. (a) Initial discharge curves, (b) dQ/dV plots of Li-rich layered $Li[Li_{0.144}Ni_{0.136}Co_{0.136}Mn_{0.544}]O_2$ oxide cells with charging at 50 °C and all the discharge process were performed at different temperatures.

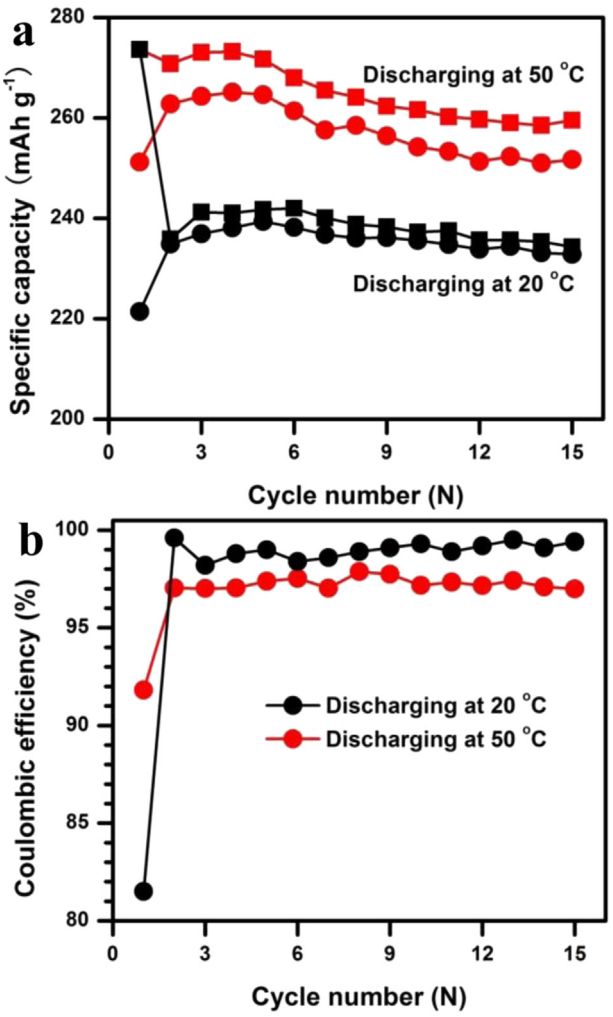

Fig. 5. (a, b) cycling capacity and coulombic efficiency at 15 cycles with charging at 20 °C.

of the latter. The other operating temperatures also show the similar trend. More importantly, the MnO_2-like component activated by charging at 50 °C is more significantly controlled by the discharge temperature (shown in Fig. 4). It is again confirmed that operating temperature can notably dominate the lithium re-intercalation into the MnO_2-like component, resulting in decrease of the initial discharge capacity and reduction of the ICE [15].

It is interesting that the ICE shows a constant value of about 92% for the cells discharged at 50 °C, even though they were charged at different temperatures. Additionally, the initial coulombic efficiency as reported before has also been compared in Table S1. For the cell charged at 0 °C, the ICE could reach 93.5%, which is due to the less Li_2MnO_3 component activated with less oxygen loss or other side reaction (Fig. 3(a)). However, this high ICE indicates that lithium ions could completely reinsert into the MnO_2-like component (Fig. 3(a)) at this temperature [12]. Thus, we speculate that the oxygen loss resulting in the irreversible capacity loss during the initial charge process may be no more than 8%, which may occur on the particle surface [17,18]. Such a small irreversible capacity loss is acceptable compared to the layered Li–Ni–Co–Mn–O oxide with the ICE less than 90% [19]. Obviously, the requirement to obtain this high ICE is to design a process which will allow lithium ions to completely reintercalate into the MnO_2-like component. The cycling performance and coulomnic efficiency with charging temperature 20 °C are also shown in Fig. 5 at pre-fifteen cycles. It is obvious that the discharge capacity at temperature 50 °C is higher about 20 mAh g^{-1} than that of the electrode at temperature 20 °C, but the average coulombic efficiency has only 97% compared to that of 99%. In addition, the typical charge–discharge curves are also illustrated in Fig. S1, S2. By comparison, it is observed that lithium ions are extracted from the electrode structure at high potentials on charge and re-inserted into the structure at lower potentials on discharge for the electrode at discharging temperature 50 °C. The great change in potential with higher discharge capacity reflects a more dramatic hysteresis, which has been brought in explaining the lower initial coulombic efficiency in Li-rich systems [20]. In addition, the electrolyte decomposition at high temperature would easily occur and lead to the lower coulombic efficiency. Therefore, lower coulombic efficiency at subsequent cycles may be closely related to this dramatic hysteresis and electrolyte decomposition at high temperature.

4. Conclusion

In this work we showed that the operation temperature played an important role for the ICE. It is certain that the process of the lithium intercalation into the MnO_2-like component derived from Li_2MnO_3 component significantly determines the ICE. Its constant value of around 92% might be a limit for this Li-rich layered Li $[Li_{0.144}Ni_{0.136}Co_{0.136}Mn_{0.544}]O_2$ oxide. This means the ICE caused by other factors, such as the oxygen loss in the lattice, might be a fixed

value with no more than 8%. Such high ICE for large scale application of Li-rich cathode material is fully acceptable. To further lower or eliminate the initial irreversible capacity loss of the Li-rich cathode, an effective way, which might directly influence this discharge process, is in progress.

Acknowledgments

The synchrotron XRD measurement was carried out at Shanghai Synchrotron Radiation Facility (SSRF) BL14B1. This work was supported financially by the Key Research Program of Chinese Academy of Sciences (Grant No. KGZD-EW-202-4), the Key Technology R&D Program of Ningbo (2012B10021) and Ningbo Science and Technology Innovation Team (Grant No. 2012B82001).

Appendix A. Supplementary data

Supplementary data related to this article can be found at http://dx.doi.org/10.1016/j.jpowsour.2014.06.031.

References

[1] J.M. Tarascon, M. Armand, Nature 451 (2008) 652–657.
[2] Z.H. Lu, D.D. MacNeil, J.R. Dahn, Electrochem. Solid State Lett. 4 (2001) A191–A194.
[3] M.M. Thackeray, S.-H. Kang, C.S. Johnson, J.T. Vaughey, R. Benedek, S.A. Hackney, J. Mater. Chem. 17 (2007) 3112–3125.
[4] T.A. Arunkumar, Y. Wu, A. Manthiram, Chem. Mater. 19 (2007) 3067–3073.
[5] H.J. Yu, R. Ishikawa, Y.-G. So, N. Shibata, T. Kudo, H.S. Zhou, Y. Ikuhara, Angew. Chem. Int. Ed. 52 (2013), 5969–5875.
[6] S.H. Yu, T. Yoon, J. Mun, S. Park, Y.-S. Kang, J.-H. Park, S.M. Oh, Y.-E. Sung, J. Mater. Chem. A 1 (2013) 2833–2839.
[7] H.J. Yu, H. Kim, Y.R. Wang, P. He, D. Asakura, Y. Nakamura, H.S. Zhou, Phys. Chem. Chem. Phys. 14 (2012) 6584–6595.
[8] C. Yu, G.S. Li, X.F. Guan, J. Zheng, L.P. Li, T.W. Chen, Electrochim. Acta 81 (2012) 283–291.
[9] C.S. Johnson, N.C. Li, C. Lefief, M.M. Thackeray, Electrochem. Commun. 9 (2007) 787–795.
[10] A.R. Armstrong, M. Holzapfel, P. Novak, C.S. Johnson, S.H. Kang, M.M. Thackeray, P.G. Bruce, J. Am. Chem. Soc. 128 (2006) 8694–8698.
[11] T. Ohzuku, M. Nagayama, K. Tsuji, K. Ariyoshi, J. Mater. Chem. 21 (2011) 10179–10188.
[12] H.J. Yu, Y.R. Wang, D. Asakura, E. Hosono, T. Zhang, H.S. Zhou, RSC Adv. 2 (2012) 8797–8807.
[13] B. Qiu, Q. Zhang, H.S. Hu, J. Wang, J.J. Liu, Y.G. Xia, Y.F. Zeng, X.L. Wang, Z.P. Liu, Electrochim. Acta 123 (2014) 317–324.
[14] B.H. Toby, J. Appl. Cryst. 34 (2001) 210–213.
[15] C. Yu, H. Wang, X.F. Guan, J. Zheng, L.P. Li, J. Alloy. Compd. 546 (2013) 239–245.
[16] Y.-K. Sun, M.-J. Lee, C.S. Yoon, J. Hassoun, K. Amine, B. Scrosati, Adv. Mater. 24 (2012) 1192–1196.
[17] B. Xu, C.R. Fell, M.F. Chi, Y.S. Meng, Energy Environ. Sci. 4 (2011) 2223–2233.
[18] H. Koga, L. Croguennec, M. Menetrier, P. Mannessiez, F. Weill, C. Delmas, J. Power Sources 236 (2013) 250.
[19] X.Y. Han, Q.F. Meng, T.L. Sun, J.T. Sun, J. Power Sources 195 (2010) 3047–3052.
[20] J.R. Croy, K.G. Gallagher, M. Balasubramanian, Z.H. Chen, Y. Ren, D.H. Kim, S.-H. Kang, D.W. Dees, M.M. Thackeray, J. Phys. Chem. C 117 (2013) 6525–6536.